

# Spice Model of Magnetic Sensitive MOSFET

Nebojsa Jankovic<sup>1</sup>, Tajana Pesic<sup>2</sup> and Dragan Pantic<sup>3</sup>

**Abstract:** A new model for a magnetic-sensitive split-drain MOSFET (MAGFET) consisting of only two NMOSTs in the equivalent sub-circuit is described in this paper. The model developed is based on the non-quasi-static (NQS) MOST model of a conventional NMOST, modified to include the effects of the Lorentz force. Based on the results of 3D numerical device simulations, it is shown that the new model can accurately predict the absolute and the relative MAGFET sensitivity for a wide range of the device biasing conditions. Unlike previous models, the new MAGFET model can also predict device dynamic response to time varying magnetic fields more realistically.

**Keywords:** Magnetic, Sensor, SPICE, Model

## I. INTRODUCTION

A magnetic sensor is a transducer which converts a magnetic field into an electric signal. Many integrated magnetic sensor circuits use a split-drain MOSFET (MAGFET) structure as a sensing device. The MAGFET is a long-channel MOSFET with a single gate and two symmetrical drains sharing the total channel current  $I_D$  [1]. An imbalance between drain currents occurs due to the influence of the perpendicular magnetic field  $B_z$ . In spite of its large offset, temperature drift and noise [1], the MAGFET remains a popular magnetic field sensing device due to its easy integration with other electronic signal conditioning blocks on silicon chips [2,3]. Hence, the ability to evaluate the performance of magnetic sensors built using MAGFETs prior to chip fabrication is essential to cost-effective development. For the accurate simulation of magnetic sensors, precise MAGFET electrical models are required that are suitable for implementation in circuit simulators such as SPICE. Until now, recent MAGFET models employed in sensor simulations [2,3] were essentially identical to the SPICE Macro Model (SMM) [4]. In the SMM approach, the MAGFET operation is emulated by the parallel connection of two conventional NMOSTs with associated external current-controlled current sources (CCCS) operating in the opposite direction [4]. The CCCS serve to produce the drain current imbalance  $\Delta i_D$  expressed as  $\Delta i_D = S \cdot I_D \cdot B_z$ , where  $S$  is the relative magnetic sensitivity and  $I_D$  is the total MAGFET drain current. A split-drain MAGFET model based on the SMM approach has also been implemented recently in the VHDL-AMS language [5].

There are two main drawbacks with the SMM approach. Firstly, the magnetic sensitivity  $S$  of the MAGFET is included as an external model parameter and its dependence on the device operating point e.g. the gate and the drain voltages  $V_{GS}$  and  $V_{DS}$ , respectively, is usually included as a polynomial approximation of measured data. Secondly, since the SMM is a static model, the dynamic MAGFET behavior in the presence of fast varying magnetic fields cannot be simulated. Both drawbacks effectively lower the accuracy of MAGFET modeling and have limited the application of the model.

To overcome these deficiencies, the authors have developed a new MAGFET model that does not involve external CCCS elements. The equivalent sub-circuit consists of only two magnetic-sensitive NMOSTs whose electrical characteristics are simulated by a modified non-quasi-static (NQS) MOST model [6,7] that includes the effects of Lorentz force. Three-dimensional (3D) numerical simulations of a MAGFET device were performed using ISE TCAD [8] to derive and evaluate the new model. The ability of the new model to predict MAGFET dynamic response to the time varying magnetic fields is also presented.

## II. 3D NUMERICAL SIMULATIONS

A split-drain MAGFET with  $L=125 \text{ nm}$ ,  $W=100 \mu\text{m}$ ,  $t_{ox}=60 \text{ nm}$  gate oxide, and substrate doping  $N_D=10^{15} \text{ cm}^{-3}$ , is studied in this paper. A concave MAGFET mask layout and standard  $1 \mu\text{m}$  CMOS technology are adopted for process simulation, yielding  $45 \mu\text{m}$  wide drain regions separated by a  $10 \mu\text{m}$  oxide gap. The internal potentials and carrier distributions of the MAGFET in presence of the perpendicular magnetic field  $B_z$  were then obtained using the 3D device simulator ISE DESSIS [8]. Fig. 1 shows the electric field distribution in the channel simulated for  $V_{GS}=5 \text{ V}$ ,  $V_{DS}=1 \text{ V}$  and  $B_z=100 \text{ mT}$ , where  $B_z$  was orientated in the  $z$ -axis direction. It can be seen that the electric field iso-lines are asymmetrical with respect to the  $(z,x)$ -plane at  $y=0$ . This asymmetry is caused by the accumulation of electrons in the upper channel region due to the influence of Lorentz force.

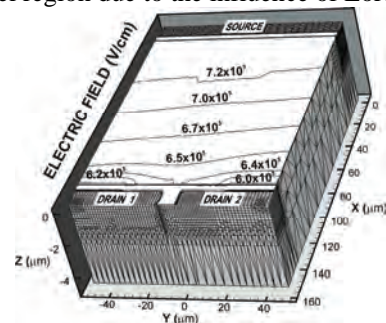


Fig.1 Electric field iso-lines in the MAGFET channel.

<sup>1</sup> N. Jankovic (E-mail: janko@elfak.ni.ac.yu),

<sup>2</sup> T. Pesic (E-mail: tatjana@elfak.ni.ac.yu), and

<sup>3</sup> D. Pantic (E-mail: panta@elfak.ni.ac.yu) are with Faculty of Electronic Engineering Nis, Aleksandra Medvedeva 14, 18000 Nis, Serbia

Let us define the steady-state excess concentration of electrons  $\Delta n$  (in units of  $\text{cm}^{-3}$ ) that is accumulated along the upper channel edge  $y = -50\mu\text{m}$  (Fig.1) as:

$$\Delta n(x, B_Z) = n(x)|_{B_Z} - n_0(x)|_{B_Z=0} \quad (2)$$

where  $n(x)|_{B_Z}$  and  $n_0(x)|_{B_Z=0}$  are the electron concentrations with and without the presence of magnetic field  $B_Z$ , respectively. For constant  $V_{GS}$  and  $V_{DS}$ , it is assumed that the same amount of electrons have been deflected from the lower channel edge  $y=50\mu\text{m}$  (Fig.1). From 3D device simulations,  $\Delta n(x, B_Z)$  was extracted at different points along the channel e.g.  $x = 30\mu\text{m}$ ,  $60\mu\text{m}$  and  $90\mu\text{m}$  corresponding to  $L/4$ ,  $L/2$ , and  $3L/4$ , respectively. The variation of  $\Delta n(x, B_Z)$  with the magnetic field  $B_Z$  extracted for constant channel positions from numerical simulations is shown in Fig. 2.

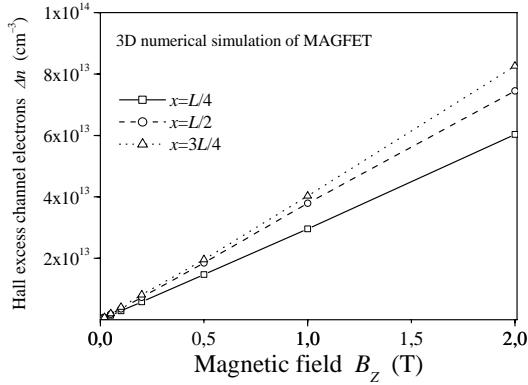


Fig.2 Excess electron concentration  $\Delta n$  versus the magnetic field  $B_Z$  extracted for different channel points at  $y=-50\mu\text{m}$ ,  $z=0$ .

A general linear dependence of  $\Delta n(x, B_Z)$  on  $B_Z$  is obtained as seen from Fig.2 and the difference  $\Delta n(L, B_Z) - \Delta n(0, B_Z)$  is noted to be small even at very high  $B_Z$ . Neglecting the latter, we can define an approximate relationship:

$$\Delta n(B_Z) \approx a \cdot B_Z \quad (3)$$

where  $a$  is a constant, of units  $\text{cm}^{-3}/\text{T}$ , whose numerical value depends on the geometry and technology of the particular MAGFET. This empirical relationship (3) forms the basis of the development of the new MAGFET model and is explained in more detail in the following section.

### III. THE MAGFET MODEL

The operation of a split-drain MAGFET is usually approximated with two identical NMOSTs operating in parallel. It is well known that the carrier transport through conventional MOSTs can be accurately modeled with the equivalent  $n$ -segment RC transmission line [6,7]. In the case of a MAGFET device, the channel transport has to be represented with two identical RC chains as illustrated in Fig. 3. Depending on the sign ( $\pm$ ) of the applied perpendicular magnetic field  $B_Z$ , the equivalent resistors  $R_k$  in one of channel chains will simultaneously decrease or increase under the action of the Lorentz force due to carrier accumulation or

depletion, respectively. In the expressions underlying the NQS MOST model [16], it can be seen that the magnitude of  $R_k$  is inversely proportional to the square root of the substrate

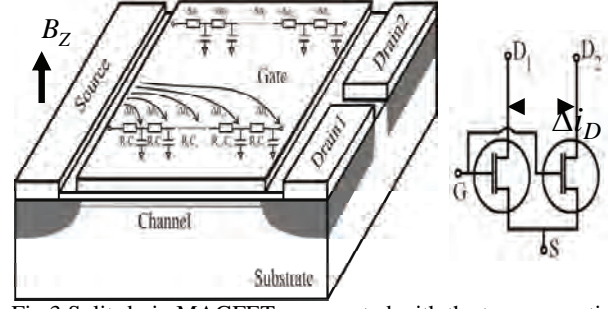


Fig.3 Split-drain MAGFET represented with the two magnetic sensitive NMOSTs

doping concentration e.g.  $\sqrt{N_{beff}}$  (see eq. (A4) in Ref [7]).

Hence, in order to include magnetic effects into the NQS MOST model [7], we will use an empirical relation (3) assuming that the magnetic field  $B_Z$  effectively modulates the parameter  $N_{beff}$  by adding or subtracting  $\Delta n(B_Z)$ . Consequently, the new effective substrate doping variable  $N'_{beff}$  will appear instead of the  $N_{beff}$  parameter in the NQS MOST model [7] as:

$$N'_{beff} = N_{beff} \pm \Delta n(x, B_Z) = N_{beff} \pm a \cdot B_Z \quad (4)$$

where the  $+$  and  $-$  signs stand for the different directions of carrier deflection in one of the NMOST channels as illustrated in Fig. 3. The relation (4) is the key modification to the NQS MOST model [7] and its efficiency in the accurate modeling of the MAGFET will be demonstrated in Section IV. The constant  $a$  appearing in (4) is a new fitting parameter for magnetic sensitivity used to calibrate the model. When  $B_Z=0$ , the MAGFET model reverts to the original NQS MOST model [7]. Unlike the SMM approach [4], the relative sensitivity  $S$  in the new MAGFET model is calculated a posteriori from simulated electrical characteristics, much the same as it is extracted during experimental MAGFET measurements.

### IV. MODELING RESULTS AND DISCUSSION

The new MAGFET model is implemented in SPICE in the form of a sub-circuit with two NMOSTs as illustrated in Fig.3. The magnetic field is represented with a separate voltage generator sourcing a voltage equal in magnitude to  $B_Z$ . This voltage source drives a special “magnetic” node in the MAGFET sub-circuit that connects  $B_Z$  with the  $N'_{beff}$  variable of the modified NQS MOST model following relation (4).

#### A. Steady-State Analysis

The new model was first calibrated to fit the electrical characteristics of a MAGFET obtained from the 3D device simulator ISE DESSIS for the case of  $B_Z=0$ . Thus, Fig.4 shows the modeled drain current imbalance  $\Delta I_D = I_{D1} - I_{D2}$

versus  $B_z$ , together with the numerical results. The experimental data of R. R.-Torres et al. [10] is also included in Fig.4 for reference. In addition, Fig.5(a) and Fig.5(b) show the dependences of the relative magnetic sensitivity  $S$  on voltages  $V_{GS}$  and  $V_{DS}$ , respectively, calculated for  $B_z = 100\text{mT}$  from the simulated electrical characteristics of the MAGFET. A good agreement is obtained between the modeling results and the numerical simulations for wide range of MAGFET biasing conditions as shown in Fig.5.

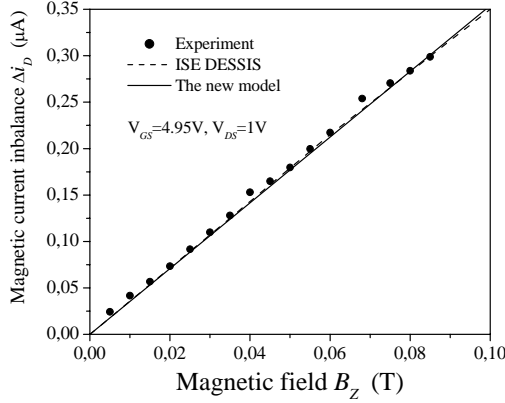


Fig.4 Comparisons of simulated, modeled and experimental MAGFET current imbalance  $\Delta i_D$  versus the magnetic field  $B_z$ . The experimental data were taken from Ref. [10].

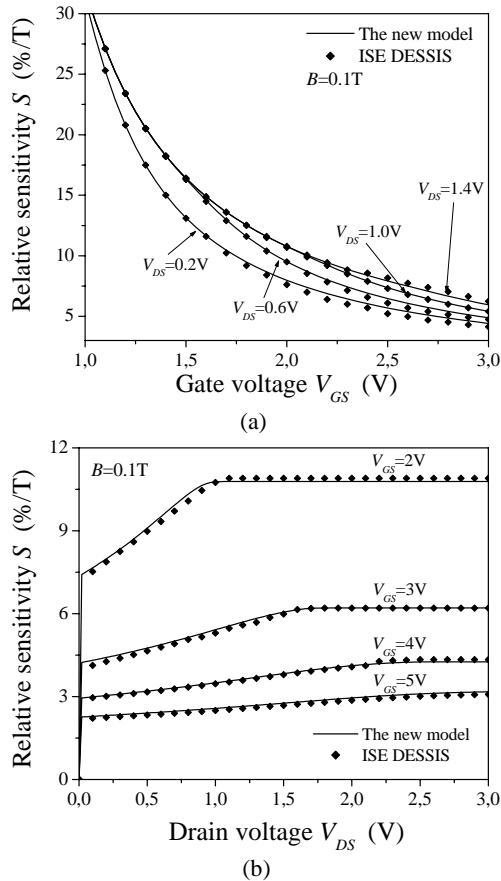


Fig.5 Relative sensitivity  $S$  of MAGFET versus: (a) the gate voltage  $V_{GS}$  and (b) the drain voltage  $V_{DS}$  extracted from 3D device numerical simulations and from the new model

### B. The MAGFET dynamic performance

Unfortunately, the present version of ISE DESSIS [8] cannot perform an electrical device simulation for the case of a time varying magnetic field  $B_z(t)$ . In addition and to the best of our knowledge, only one set of experimental data has been published in relation to the dynamic performance of split-drain MAGFETs under the influence of a pulsed magnetic field [9]. Consequently, we can only demonstrate here the advantages of the new MAGFET model over the SMM approach [4] in predicting MAGFET dynamic behavior. For proper comparison, the NMOSTs of the SMM [4] are taken to be identical to the ones used in the sub-circuit of the new MAGFET model. Also, in order to obtain the same maximal  $\Delta i_D$  response in both models, the relative sensitivity  $S$  found for given values of  $B_z$ ,  $V_{GS}$  and  $V_{DS}$  in the new MAGFET model simulations were subsequently used as the pre-requested input parameter of the SMM [4].

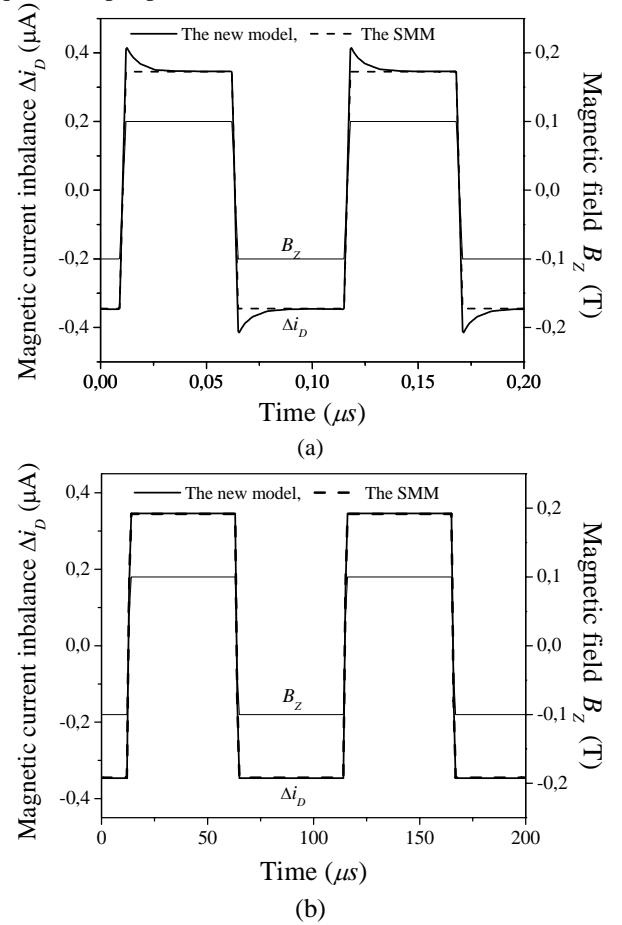


Fig.6 Drain current imbalance  $\Delta i_D$  of MAGFET simulated with the new model and with SMM in case of pulsed  $B_z$  signal with: (a) 3ns rise/fall times and (b)  $1\mu\text{m}$  rise/fall times.

Let us assume that the MAGFET is subjected to an extremely steep  $B_z$  pulsed signal with 3ns rise/fall times. Then, the simulated pulsed response  $\Delta i_D(t)$  is as shown in Fig. 6.a. As it can be seen, the new MAGFET model yields transient peaks in the simulated response, whereas these peaks do not appear in the  $\Delta i_D(t)$  pulses obtained with the SMM [4].

Note that the  $\Delta i_D(t)$  peaks would be expected in reality due to

the transient charging of channel distributed capacitance before reaching steady-state conditions. This conclusion can be indirectly confirmed from the results shown in Fig.6.b. Namely, for substantially slower  $B_Z$  pulses, the transient peaks are small, becoming negligible if plotted on a long time-scale. Hence, the device response  $\Delta i_D(t)$  from the new MAGFET model to the slow  $B_Z$  pulses with  $1\mu s$  rise/fall times and the response of the SMM [4] will be in better agreement as shown in Fig.6.b.

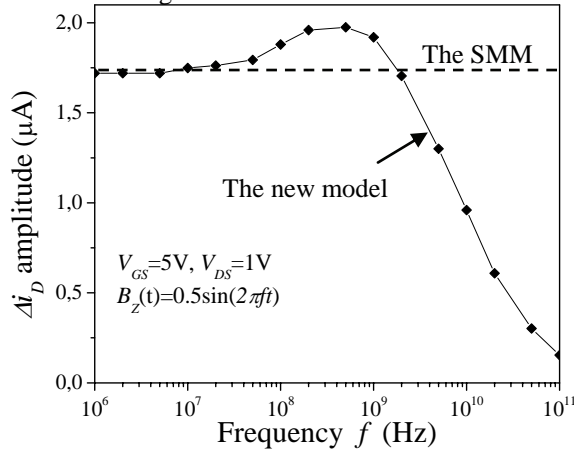


Fig.7 Drain current imbalance amplitude  $\Delta i_D$  of MAGFET versus frequency  $f$  in case of the sine-wave magnetic signal  $B_Z$  simulated with the new model and with SSMM.

Fig.7 shows the simulated frequency characteristics of the  $\Delta i_D(t)$  response obtained for  $V_{GS}=5V$  and  $V_{DS}=1V$  from the new MAGFET model. For the purposes of the simulation, a sine-wave magnetic field of  $B_Z = 0.5 \cdot \sin(2\pi \cdot f \cdot t)$  in units of Tesla with variable frequency  $f$  is assumed. Fig.7 clearly indicates the existence of some limiting frequency  $f_i$  for which the MAGFET sensitivity drops to zero. In contrast, the SMM [4] is not able to predict any frequency response limitations of MAGFET sensitivity as illustrated by the dashed line in Fig.7. It is important to emphasize that the limited bandwidth of MAGFET sensitivity is a more natural simulation result, since  $f_i$  commonly appears in the sensitivity characteristics of other sensors in different signal domains [12]. A rather high  $f_i$  of around 70 GHz is predicted in Fig.7 in the new model, most likely due to the assumption of an ideal MAGFET device. A much lower  $f_i$  would be expected due to the influence of the device geometry, noise, and offset [13] as well as the presence of parasitic RC elements in practical MAGFETs. These non-idealities are not included in the present model. The model also predicts a slight increase of  $\Delta i_D(t)$  appearing at high frequencies of  $B_Z$  as shown in Fig.7. From the Fourier analysis, we found that the  $\Delta i_D(t)$  sine-wave response of MAGFET in case of large  $B_Z$  swing has been distorted at high frequencies by the appearance of additional harmonics which slightly increases the overall output signal amplitude. Since, for small amplitude of  $B_Z$  signal the  $\Delta i_D(t)$  overshoot is negligible, we can attributed this effect to the highly nonlinear model equations describing the RC elements. Whether the effect exists in practical device frequency characteristics or it

stems from model approximations can be only verified by the experiments.

## V. CONCLUSIONS

A new MAGFET model consisting of only two magnetic sensitive NMOSTs in the equivalent sub-circuit is described in this paper. The new model developed is based on the non-quasi-static (NQS) MOST model of conventional NMOSTs, modified to include the effects of Lorentz force. Based on 3D numerical device simulations, it is shown that the new model can accurately predict the absolute and relative MAGFET sensitivity for different biasing conditions of the device. It is also shown that unlike the widely used SMM, the new MAGFET model is able to simulate the device dynamic response to time varying magnetic fields far more realistically.

## REFERENCES

- [1] R.S. Popovic, *Hall Effect Devices*, Taylor & Francis; 2<sup>nd</sup> edition (2003)
- [2] C. Rubio, S. Bota, J.G. Macias, J. Samitier, "Monolithic integrated magnetic sensor in a digital CMOS technology using a switched current interface system", *Proc. IEEE Instrumentation and Measurement Technology Conference*, 2000, pp. 69-73
- [3] C. Rubio, S. Bota, J. G. Macias and J. Samitier, "Modelling, design and test of a monolithic integrated magnetic sensor in a digital CMOS technology using a switched current interface system", *Journal of Analog Integrated Circuits and Signal Processing*, Vol. 29, 2001, pp. 115-126
- [4] Shen-Iuan Liu Jian-Fan Wei Guo-Ming Sung "SPICE macro model for MAGFET and its applications" *IEEE Transactions on Circuits and Systems II: Analog and Digital Signal Processing*, Volume: 46, 1999, pp. 370-375
- [5] M. Zawieja, A. Napieralski, J. J. Charlot, "Application of VHDL-AMS Language for simulation of magnetic sensors", *Proc. TCSET'2002*, Lviv - Slawsko, Ukraine, 2002, pp 345-349
- [6] T. Pesic T, N. Jankovic "Physical-based non-quasi static MOSFET model for DC, AC and transient circuit analysis", *Proc. 24th International Conference on Microelectronics, MIEL'04*, Vol. 1: 2004, pp. 261-264
- [7] T. Pesic T, N. Jankovic, "A compact non-quasi-static MOSFET model based on the equivalent non-linear transmission line", *IEEE Trans. on Computer-Aided Design of Integrated Circuits and Systems*, Vol.24, 2005, pp. 1550-1561
- [8] ISE TCAD – Users Manual, Release 7.0, *Integrated System Engineering AG*, Zurich, Switzerland
- [9] E. A. Gutierrez-D, E. Torres-R, T, R. Torres, "Magnetic sensing as signal integrity monitoring in integrated circuits", *Proc. of Solid-State Device Research Conference (ESSDERC '05)*, Grenoble, France, 2005, pp. 277 – 280
- [10] R. R.-Torres, E. A. G.-D., R. Klima, S. Selberherr, "Analysis of split-drain MAGFETs", *IEEE Trans. Electron Devices*, Vol. 51, No. 12, 2004, pp. 2237-2245
- [11] J. W. Nilsson and J. R. Evans, *PSpice Manual Using Orcad Release 9.2 for Introductory Circuits*. Upper Saddle River, NJ: Prentice-Hall, 2002
- [12] S. Soloman, *Sensors Handbook*, McGraw-Hill Professional (1998)
- [13] G.-M. Sung and S.-I. Liu, "Error correction of transformed rectangular model of concave and convex MAGFETs with AC bias", *IEE Proc.-Circuits Devices Syst.*, Vol. 151, No. 6, 2004, pp.593-600